

Location of Ryanodine Receptor Binding Site on Skeletal Muscle Triadin[†]Anthony H. Caswell,* Howard K. Motoike,[‡] Hongran Fan,[§] and Neil R. Brandt*Department of Molecular and Cellular Pharmacology, University of Miami School of Medicine,
1600 N.W. 10th Avenue, Miami, Florida 33136**Received June 2, 1998; Revised Manuscript Received October 27, 1998*

ABSTRACT: The binding between intact triadin or expressed triadin peptides and the ryanodine receptor has been investigated using membrane overlay and affinity chromatography. Ryanodine receptor binds to triadin blotted onto nitrocellulose with a K_D of 40 nM in a medium containing 150 mM NaCl. The binding is substantially inhibited by hypertonic salt solution. Blot overlay experiments show that ryanodine receptor binds to bacterially expressed peptides, triadin(110–280), triadin(110–267), and triadin(279–674), but to no other moieties of the protein (numbers in parentheses are the residue positions). This binding is strongly inhibited by hypertonic salt solution. The same three triadin peptides as well as triadin(68–267), when attached to a glutathione column, bind to the ryanodine receptor. However, triadin(110–280) binds with high affinity, while triadin(68–267), triadin(110–267), and triadin(279–674) bind with low affinity. Triadin(258–280), triadin(267–280), and triadin(258–299) all bind to the ryanodine receptor with high affinity. On the other hand, a construct containing triadin(267–280), but preceded by nine residues of heterologous amino acids, does not bind significantly. These observations indicate two types of binding between triadin and the ryanodine receptor: (1) a low-affinity ionic interaction of large portions of triadin; (2) a specific high-affinity binding of a short relatively hydrophobic segment. The binding of this segment is probably the physiologically important domain for attachment between triadin and the ryanodine receptor.

The mechanism of skeletal muscle activation is still not known. Two major proteins are known to play an important role in signaling between the T tubule¹ and the TC of the SR. The DHP_r in the T tubule senses the membrane potential and transmits a signal of depolarization to the TC (1, 2). Chimeric DHP_r with a cardiac backbone and skeletal II–III cytoplasmic loop is able to rescue contraction in dysgenic mice in the absence of calcium entry (3). The Ryr receives the message from the DHP_r and opens its channel to release Ca²⁺ from the lumen into the cytoplasm (4–6). Freeze–fracture electron micrographs indicate arrays of intercalated particles in the T tubule in register with rows of shallow projections from the TC. These have been interpreted to indicate that the DHP_r in the T tubule overlies the Ryr in the TC and is sufficiently close to make direct contact (7).

Direct binding between the DHP_r and Ryr has not been observed. DHP_r and Ryr, coexpressed in Chinese hamster ovary cells, do not coassociate (8). Moreover, cell lines from genetically defective mice, which do not contain the Ryr, form junctions containing filamentous bridging material (9).

Similarly, cell lines from dysgenic mice that are missing the α_1 subunit of the DHP_r are able to form triad junctions (10). A discrete portion of the II–III cytoplasmic loop of the DHP_r has been identified which may interact with the Ryr (11–13). Recently a binding region of the Ryr has been identified that binds to the DHP_r II–III loop (14). Although these studies may identify a site of physiological coupling between the DHP_r and the Ryr, the structural integrity of the triad junction depends on high-affinity binding between intact proteins in the T tubule and SR.

Our studies of junctional proteins have indicated the presence of a protein, triadin, which, in binding assays of dissolved proteins, associates with both the DHP_r and Ryr (15–17). This glycoprotein is an intrinsic protein of the TC that forms a disulfide-linked homopolymer of variable, but large, size (18). The protein has a monomeric molecular mass of 79 kDa and contains a single hydrophobic segment of sufficient length to cross the membrane as an α helix (19, 20). The rest of the molecule is heavily charged with a preponderance of lysine residues. However, three short segments are more hydrophobic in character, and one of the controversies of the protein concerns the membrane disposition of these regions in determining the peptide topology. We have proposed that these segments span the membrane (21), while others have argued that they are entirely luminal (22, 23). Two cysteines are present in rabbit skeletal muscle triadin, both of which must form intermolecular disulfides in order to account for the polymerization of triadin. The disulfide linkages occur through bonding between identical cysteines on neighboring molecules (24).

The evidence that triadin binds to the Ryr was originally adduced on the basis of the binding in Western blot overlay

[†] Supported by NIH Grant AR43355.

[‡] Present address: Institute of Molecular Pharmacology and Biophysics, University of Cincinnati College of Medicine, 231 Bethesda Ave., P.O. Box 670828, Cincinnati, OH 45267-0828.

[§] Present address: Department of Dermatology, Stanford University Medical Center, 1201 Welch Rd., MSLS Building, Room P252, Stanford, CA 94305.

¹ Abbreviations: T tubule, transverse tubule; TC, terminal cisterna; SR, sarcoplasmic reticulum; DHP_r, dihydropyridine receptor; Ryr, ryanodine receptor; CHAPS, 3-[(3-cholamidopropyl)dimethylammonio]-1-propanesulfonate; PMSF, phenylmethylsulfonylfluoride; GST, glutathione-S-transferase; PBS, phosphate-buffered saline; DMSO, dimethyl sulfoxide; MOPS, 3-(N-morpholino)propanesulfonic acid; IPTG, isopropyl- β -D-thiogalactopyranoside.

of the intact isolated Ryr onto triadin. The observation was confirmed by attaching isolated triadin to an affinity support and observing the specific retention of Ryr from detergent-dissolved triads on the column (16). These observations have been confirmed using triadin(100–706) expressed in bacteria (25). Evidence of binding of triadin to the Ryr in situ is confined to the observation that triadin detected using immunogold particles in intact SR vesicles is in immediate juxtaposition to cytoplasmic protrusions identified as junctional feet (26). This observation indicates a close association of these two proteins, but does not prove that they bind directly. Immunolocalization experiments show that triadin and DHPr colocalize at the limits of resolution of immunofluorescence microscopy in the muscle even when the Ryr is not expressed (9).

In this paper, we have addressed more closely the binding of triadin to the Ryr using both intact triadin and expressed peptides of portions of the molecule. We have examined the extent of ionic interaction through the effect of varying the salt concentration of the binding buffer and conclude that, while considerable binding may occur through nonspecific charge attraction, there is also a specific component of binding confined to a short segment of triadin.

METHODS

Preparation and Labeling of Ryanodine Receptor. TC/triads were prepared from rabbit sacrospinalis muscle as described before (27). The fraction from the density gradient centrifugation was diluted into 1 M KCl and pelleted to extract glycolytic enzymes which are attached to the vesicles. Ryr was extracted from the preparation (7 mg/mL) with 1.4% CHAPS/0.14% phosphatidylcholine in 1 M KCl, 10 mM Tris-HCl, 50 mM potassium phosphate, pH 7.4. This and all subsequent media included, unless otherwise stated, 200 μ M PMSF, 1 μ M leupeptin, and 1 μ M pepstatin protease inhibitors. Ryr was purified in two stages through a hydroxyapatite column followed by a heparin–agarose column according to the method of Brandt et al. (16). Ryr was labeled with 125 I using the Bolton–Hunter reagent. Either iodination was performed after the hydroxyapatite column and before the heparin column or it was performed on the heparin column eluate. The elution from the column immediately before labeling included only PMSF as protease inhibitor. In the former case, the heparin column was used to separate iodide and small reaction products from the Ryr, while in the latter case the reaction was followed by two successive 1 mL spin columns [1 mL Sephadex G-50 equilibrate with 0.2% CHAPS in Dulbecco's PBS (Gibco/BRL)].

Bolton–Hunter reagent (Pierce) was dissolved at 2 mg/mL in DMSO and diluted 2000-fold into 50 μ L of 50 mM NaHPO₄, pH 7.4, containing 0.5 mCi (629 GBq/mg) of Na 125 I in an Iodogen-coated (Pierce) Eppendorf microfuge tube. After 30 s, the reaction mixture was transferred to a clean microfuge tube containing 50 μ L of Ryr (2–10 μ g) in the output from the hydroxyapatite column (15 mL of 200 mM KPO₄, 0.2% CHAPS, and 100 μ M PMSF) or the heparin column (0.6 M NaCl, 0.02 M Na-MOPS, pH 7.4, 0.2% CHAPS, and 100 μ M PMSF). The coupling reaction was allowed to progress for 30 min at 4 °C and was then quenched by addition of Tris-HCl (20 mM, pH 7.4), *p*-hydroxyphenylacetic acid (2 mM), and KI (2 mM).

Spot Blots. Either TC/triads or junctional face membrane was employed in this assay. The latter was prepared by treating 50 mg of TC/triads with Triton X-100 (2 mg/mg of protein) in the presence of 5 mM Tris–EGTA, pH 7.4, and centrifuging through a linear sucrose gradient (12.5–65% w/w). The opaque suspended material in the gradient was removed, diluted, and pelleted.

Vesicles (1.6 mg/mL) were dissolved in 1.4% CHAPS, 0.14% phosphatidylcholine, 1 M NaCl, 2.5% β -mercaptoethanol, 10 mM Tris-HCl, pH 7.4. This medium dissolves and separates triadin from Ryr and converts triadin into its monomer. The solution (25 μ L) was applied using a Hamilton syringe to a nitrocellulose filter and dried using warm air from a drier. Each spot of 1–1.5 cm was cut out and blocked with 1 mL of 3% bovine serum albumin or 1% casein in 200 mM NaCl, 20 mM Tris-HCl, pH 7.4, overnight in 5 mL plastic sample cups. The filters were then washed with the same salt solution as used in the incubation. Labeled Ryr was incubated with the filters in a volume of 0.25 mL for 3 h at room temperature in 20 mM Tris-HCl, 0.5% CHAPS, 0.05% phosphatidylcholine, 1 mM Tris–EGTA, and salt as described in the figures. This was followed by washing 3 times with 20 mM potassium gluconate, 20 mM Tris–MOPS. The sample was air-dried and counted in a γ counter. Control samples were filters that had been spotted without triads, but were otherwise treated and incubated with Ryr in the same manner as the samples. Controls were run at each salt concentration used for the sample.

Triadin Constructs. All the constructs are based on GST fusion protein and contain, in addition to GST, a segment which allows protein kinase A labeling (not used here), followed by a five glycine repeat to allow conformational uncoupling of GST from the insert (28). The various triadin constructs were formed using restriction digests from parent fusion peptides that had been produced by PCR as described (21). The position along the triadin molecule of the fusion peptides is shown in Figure 1. This figure shows salient features of triadin along the top including the long hydrophobic segment (in large box) that is believed to cross the membrane. In addition, there are three short regions of relatively hydrophobic amino acids (small boxes) two of which contain cysteines (C-), which are responsible for the polymerization of triadin. Since most of the fusion peptides have been constructed by insertion into the polylinker region using restriction digests, there is a short leader sequence between the glycine repeat and the triadin sequence and a terminal sequence from the polylinker before the end of translation. The line indicates the position and length of the triadin peptide, while the letters designate the leading amino acids after the poly-Gly and the terminating amino acids. The thickness of the line designating the construct is used to designate the strength of binding of the construct to the Ryr as described under Results.

Preparation of GST Fusion Proteins. GST fusion protein constructs were transformed into competent *E. coli* BL2 cells and plated on ampicillin plates. Colonies were tested for fusion protein expression after induction for 2 h with 0.6 mM IPTG and, then, streaked on ampicillin agar. Multiple 5 mL LB broth–ampicillin cultures were inoculated from the streak plate and grown to mid-log phase (2–3 h) at 37 °C. The number of cultures inoculated and used was determined by the ability of the construct to produce fusion

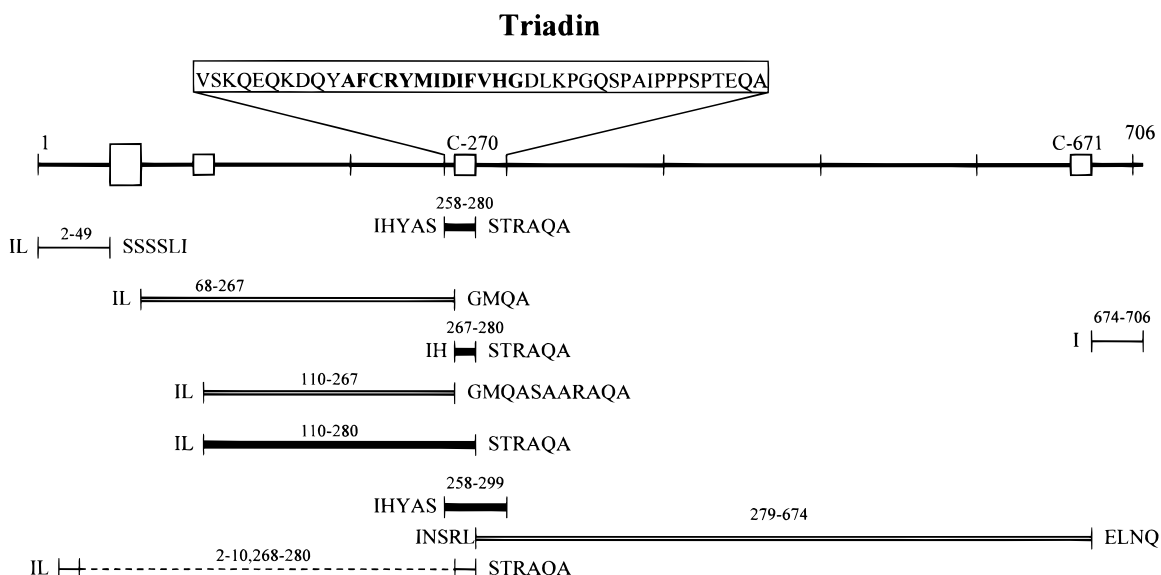


FIGURE 1: Structure of triadin and of triadin fusion protein constructs. The top line shows features of triadin including the long hydrophobic segment represented by the large box and the three short hydrophobic segments represented by the small boxes. The vertical bars indicate each 100 amino acids. The boxed sequence refers to the amino acids adjacent to cysteine 270 which are contained in the short expression constructs shown below. The boldface characters represent the sequence from 268 to 280. The rest of the figure shows the position and length of the expression constructs. The bars at the end of each line indicate the position on the triadin line of the N and the C terminus of the insert. The constructs are identified in the text and above each line by the amino acid numbers of the insert. The amino acids before and after the bars represent heterologous amino acids introduced in the fusion construct between the poly-Gly and the stop signal. The binding affinity of the constructs is indicated by the type of horizontal line: thick solid lines delineate high-affinity binding; intermediate open lines indicate low-affinity binding, while thin lines indicate absence of significant binding.

protein relative to the GST parent vector. Fusion protein production was induced by addition of 0.6 mM IPTG. After 2 h, the bacteria were harvested and resuspended in 1.8 mL of lysis buffer [500 mM NaCl, 50 mM Na₂HPO₄, pH 7.4, 1 mM EDTA, 1 mM DTT, 0.1% Tween 20, and protease inhibitors (Mintabs minus EGTA, Boehringer-Mannheim)]. Bacteria were disrupted by two passes through a French press minicell at 8000 psi. Cell debris was removed by centrifugation and the extract incubated for 30 min at 4 °C with 0.15–0.2 mL of glutathione–sepharose (Pierce) preequilibrated with the lysis buffer. The gel beads were washed 5 times with lysis buffer and stored at 4 °C in lysis buffer. The amount of each fusion protein bound to the beads was estimated by Laemmli gel electrophoresis, and all constructs were equalized by adjustment of the gel to lysis buffer ratio. Routinely the amount of fusion protein used for each assay was in the range of 500 ng as estimated against a BSA standard curve. New transformations were carried out at least once a month.

Binding to GST Fusion Peptides. Western blot overlays were performed as described previously. For the GST fusion protein, glutathione–Sephadex was boiled 3 min in 2 volumes of solubilizing buffer, electrophoresed on Laemmli slab gels, and blotted to Immobilon (Millipore) in a Genie semi-dry apparatus (Ideal Scientific). Blots were blocked with 1% casein in PBS and washed into overlay medium (200 mM NaCl, 20 mM MOPS, pH 7.4, 0.2 mM CaCl₂, 0.2% CHAPS).

Binding reactions of GST fusion protein to glutathione–Sephadex were carried out in triplicate in 0.1 mL reaction volumes in media adjusted to 20 mM MOPS, pH 7.4, 0.5 mM CaCl₂, 0.2 mM EDTA, 1 mM DTT, 0.2% CHAPS, and 50 000–200 000 cpm of [¹²⁵I]-Ryr in Eppendorf microfuge tubes. The concentrations of NaCl and unlabeled Ryr are

indicated in the figure legends. Binding was carried out for 2–3 h at 20 °C with constant mixing and the reaction mixture then transferred to minicolumns with 1 mL of reaction buffer. Columns were washed 3 times with 1 mL of reaction buffer, vacuum-dried, and counted in a γ counter. All constructs were analyzed in two or more independent experiments.

RESULTS

Binding of Ryr to Triadin from Triadic Vesicles. The binding of the Ryr with triadin has been described previously, but the methods were not well adapted for multiple assays (16). Here we have used spot blots of triads or junctional face membrane in order to allow a large number of samples and conditions to be examined. In this approach, vesicles are dissolved in order to effect physical separation of Ryr from triadin. This should allow triadin to attach to the filter separately from the endogenous Ryr and so allow free interaction of the protein with the purified, labeled Ryr. The triadic vesicles have been washed with salt in order to extract glycolytic proteins that bind to the Ryr (15). Figure 2A shows the purity and labeling specificity of the Ryr. Two bands are observed toward the top of the gel which correspond to the size of intact Ryr and to a product of proteolytic cleavage which can probably be attributed to endogenous calpain (lane 1). The iodine label is present in this protein and cleavage product (lane 2). Figure 2B shows a Western blot and overlay of TC/triads. The immunoblot with anti-triadin antibody indicates a predominant band at approximately 95 kDa with two higher bands that probably reflect incompletely depolymerized triadin (lane 1). The overlay with labeled Ryr indicates binding to a single band of the same molecular mass as triadin (lane 2). The high specificity of interaction in this preparation of salt-washed triads indicates that triadin

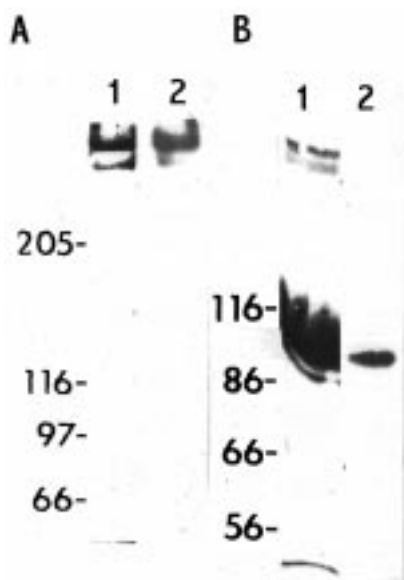


FIGURE 2: Labeling and overlay of Ryr onto TC/triads. (A) Lane 1: Coomassie blue stain of purified Ryr showing two bands corresponding to intact Ryr and cleavage product. Lane 2: Autoradiograph of label of the purified Ryr showing label in the parent protein and cleavage product. (B) Lane 1: Immunoblot of TC/triads using mAb GE4.90 against triadin showing one major band of monomeric triadin. The bands toward the top of the gel are polymeric triadin that was not reduced by the sample buffer. Lane 2: Overlay with labeled Ryr showing labeling of a single band corresponding to the position of triadin. The medium for the incubation contained 20 mM NaCl, 20 mM potassium gluconate, 20 mM Tris-MOPS, 0.5% CHAPS, 0.05% phosphatidylcholine. Incubation was for 3 h at room temperature and was followed by four washes with the incubation medium (without Ryr).

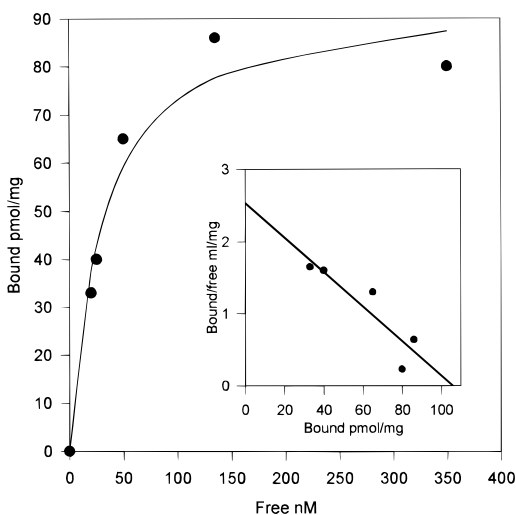


FIGURE 3: Binding of Ryr to junctional face membrane. Vesicles were spotted onto nitrocellulose membranes, blocked, and incubated with Ryr as described under Methods. [125 I]-Ryr was incubated with the membranes in the presence of varying concentrations of unlabeled Ryr in the presence of 150 mM NaCl, washed, and counted as described under Methods. The concentration of labeled Ryr was added to that of the added unlabeled protein in order to calculate the total protein. The affinity and number of binding sites are calculated from the Scatchard plot (inset). The binding curve is based on a regression fit to a bimolecular binding function.

is the predominant binding protein of the Ryr in the preparation.

Figure 3 is a binding plot of Ryr on the junctional face membrane as a function of Ryr concentration using spot

blots. The data show that binding is saturable in the presence of a physiological concentration of salt (150 mM). The Scatchard plot (insert) shows, within the limits of variability of the data, a single type of binding site with a K_D of 40 nM Ryr tetramer and 100 pmol/mg maximal number of binding sites. We are assuming that only one of the subunits of the Ryr is able to bind to triadin in this solid phase assay, since the geometry would need to be very exact to allow a second binding interaction. The binding affinity is similar to that of other proteins that bind to each other, but are not associated as subunits. The number of binding sites may be an underestimate of the true value since some triadin molecules attached to the filter may not be accessible to the Ryr. The Ryr tetramer density on TC/triads is approximately 20 pmol/mg based on ryanodine binding. The density should be significantly higher on junctional face membranes, since the Triton X-100 extracts nonjunctional proteins such as the calcium ATPase. The number of binding sites observed here is consistent with a slight excess of triadin monomer over the Ryr as has been reported elsewhere (18, 19).

The specificity of binding of the Ryr to triadin was investigated further by incubating the proteins in the presence of varying concentrations of salt in spot blots (Figure 4A) and Western blot overlays (Figure 4B). Figure 4A shows that salts inhibit binding of labeled Ryr to the spots (solid circles), although the inhibition appears to be incomplete. When a higher concentration of Ryr was incubated by adding a 7-fold excess of unlabeled Ryr, the binding was almost independent of salt concentration (open squares).

The gel overlay (Figure 4B) shows the same effect. Specific binding to the triadin band decreases at high ionic strength. Nevertheless some binding still occurs when the Ryr is incubated in a medium that contains 500 mM NaCl. The figure shows that ionic interactions are contributing to the protein binding at low salt concentrations, but binding is still retained in hypertonic media, indicating a specific interaction.

Binding of Ryr to Expressed Triadin Peptides. To refine the binding site of triadin onto the Ryr, we have expressed several peptides corresponding to partial sequences of the molecule. These have been expressed as fusion peptides using glutathione transferase as the carrier in order to facilitate purification of the proteins from the bacterial lysate and because the carrier increases the solubility of some of the peptides. The topology of triadin in the membrane is still controversial, but we have devised peptides to correspond to likely domains of the protein. For this reason, most of the peptides synthesized are bounded by or about the hydrophobic segments. The regions have been designated as shown in Figure 1. We have attempted to avoid peptides which would segregate contiguous regions that vary strongly in their charge distribution, since this may give rise to artifactual binding. For example, we have not synthesized peptides which separate residues 118–139, which are strongly acidic, from the following residues 140–267 which are largely basic.

Figure 5 shows a Western blot overlay of Ryr onto GST fusion proteins purified from bacterial lysates on a glutathione column and then eluted in SDS gel sample buffer and electrophoresed. Figure 5A shows the protein staining of the gel that indicates the relative protein content in each lane. The column has extensively purified the proteins.

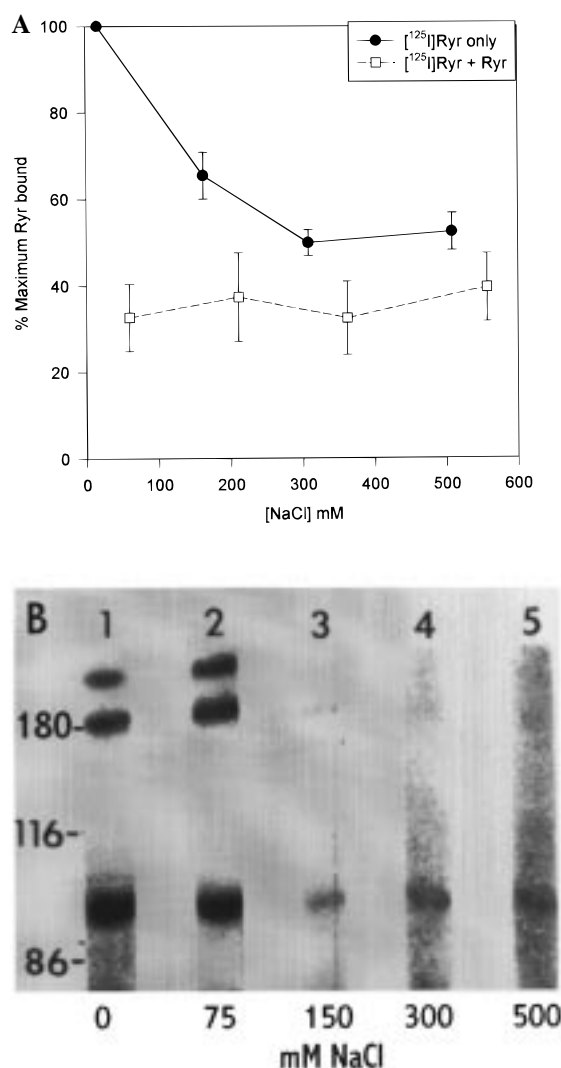


FIGURE 4: Effect of ionic strength on binding of Ryr to TC/triads. (A) Spot blot: Solid circles are labeled Ryr alone, while the open squares are in the presence of 7-fold excess of unlabeled Ryr. The error bars are the standard error of the means of three separate experiments. Data are normalized with reference to the binding in the absence of added unlabeled Ryr at the lowest salt concentration. (B) Western blot overlay of Ryr onto TC/triads at varying concentrations of NaCl.

Bacterial proteins are largely absent from the gel since the minor bands present are specific for each construct. Some of the expressed peptides have undergone limited hydrolysis, but the major band in each case represents the intact peptide. The larger peptides are toxic to the bacteria and cause cessation of growth in induced cultures. In this and subsequent experiments, we have attached as nearly as possible the same amount of protein to the column for each construct. Figure 5B–D shows the Ryr overlays performed in the presence of 100 mM (Figure 5B), 200 mM (Figure 5C), and 400 mM (Figure 5D) NaCl. In the lowest ionic strength medium, the larger constructs, (110–267), (110–280), and (279–674), all bind strongly to the Ryr. The most potent of these is (279–674) in which both the parent peptide and the products of proteolysis react strongly. In contrast, no binding was observed to the GST construct by itself or to the N- and C-terminal peptides (2–49 and 674–706) or the small constructs in the region 258–299. We have also tested the overlay of the N- and C-terminal constructs in the presence

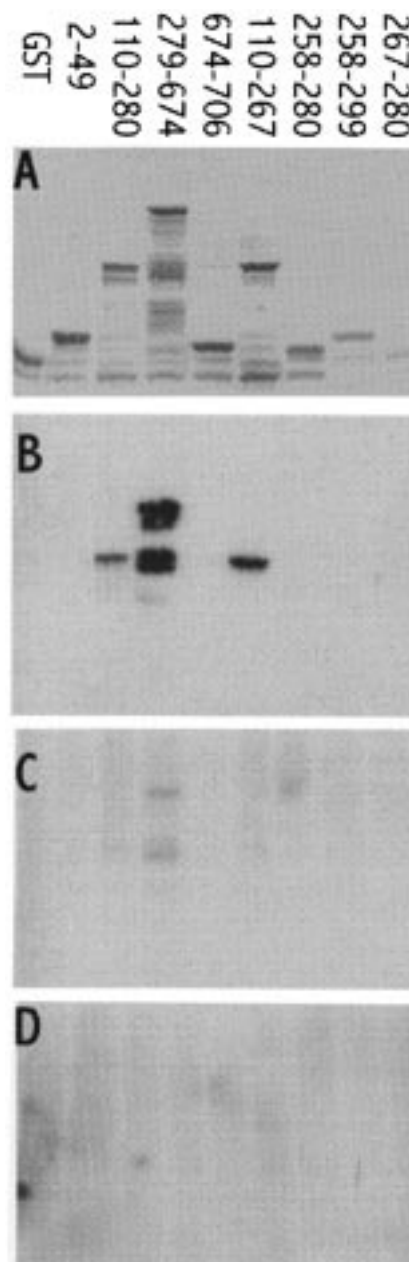


FIGURE 5: Overlay of Ryr onto triadin fusion peptides. The purification of the peptides on the glutathione column is described under Methods. (A) The peptides were eluted in SDS sample buffer and developed using Coomassie brilliant blue. The numbers above each lane refer to the triadin residues in the construct as diagrammed in Figure 1. The molecular mass of the parent GST construct is 28 kDa. The intact fusion peptide in each lane is the slowest running visible band. (B, C, and D) Western blot overlay in 100 mM, 200 mM, and 400 mM NaCl, respectively. Techniques are described under Methods. The lanes correspond to those of (A). The blot was incubated for 3 h at room temperature with the Ryr and then washed in the same medium 5 times in a total time period of 20 min.

of media that activate (100 μ M CaCl_2) or inhibit (1 mM EGTA, 1 mM MgCl_2) the opening of the Ca^{2+} release channel without observing any binding. The overlays in the higher ionic strength media show greatly diminished binding with no residual binding in 400 mM NaCl. This is consistent with a predominantly ionic interaction. These peptides have a very high component of charged and ionic residues. Triadin(279–674) contains a preponderance of cationic sites

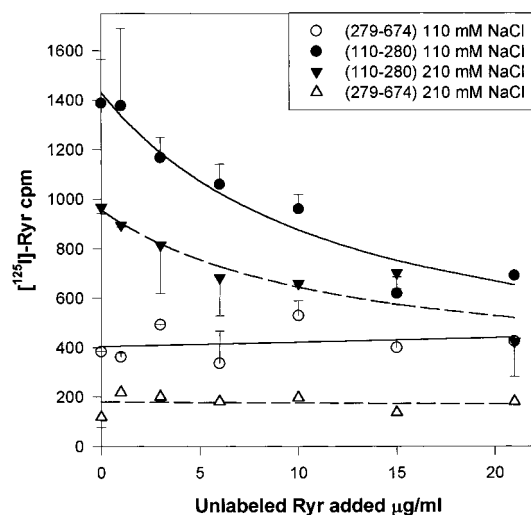


FIGURE 6: Binding of Ryr to triadin peptides at different ionic strengths. The preparation of the constructs and affinity attachment to the column are described under Methods. The column was incubated with Ryr for 3 h in the media described under Methods except that the salt concentration was as shown in the figure. The error bars represent the range of duplicate measurements. The plots and regression lines were produced using Sigmaplot. The regression lines corresponding to the solid symbols are hyperbolic binding curves with a constant binding superimposed. The regression lines corresponding to the open symbols are linear.

which may account for its potency of binding to the acidic Ryr.

The detection of binding between proteins by Western blot overlay is simple and effective, but is not quantitative. It may fail to detect binding that requires normal folding of the protein backbone or in which the binding site is occluded by binding of the electrophoresed protein to the membrane support. We have used glutathione columns both to purify fusion peptides and to attach them to a solid support. Ryr is incubated directly with the gel followed by rapid washing through a manifold. The gel is then counted in a γ counter.

The GST construct by itself or the glutathione column without fusion peptide retains little or no Ryr. Sometimes a low level of retention is observed which is unaffected by the addition of unlabeled Ryr. This may reflect binding to the column of free iodide which was not completely removed from the Ryr during purification. Binding of Ryr to the naked GST construct has been subtracted from all sample counts, since the GST is present in all constructs. We have confirmed that the N- and C-terminal peptides (2–49 and 674–706) do not bind significantly to the Ryr in the presence of either 100 μ M Ca^{2+} or 1 mM EGTA. The larger constructs (68–267, 110–267, 110–280, and 279–674) all bind significantly. These data confirm the overlay data, but other observations reveal a new class of binding to the Ryr.

Figure 6 shows the effect of increasing concentrations of unlabeled Ryr on the binding of [^{125}I]-Ryr to the triadin constructs, 110–280 and 279–674, in media containing two different salt concentrations. Binding of label to triadin(110–280) is considerably diminished by unlabeled Ryr, indicating a high-affinity binding site for this construct both in 110 mM NaCl and in 210 mM NaCl. The overall binding is diminished in the higher salt concentration, but the inhibition by cold Ryr is largely unaltered. This suggests that, in addition to the high-affinity binding site, a second low-

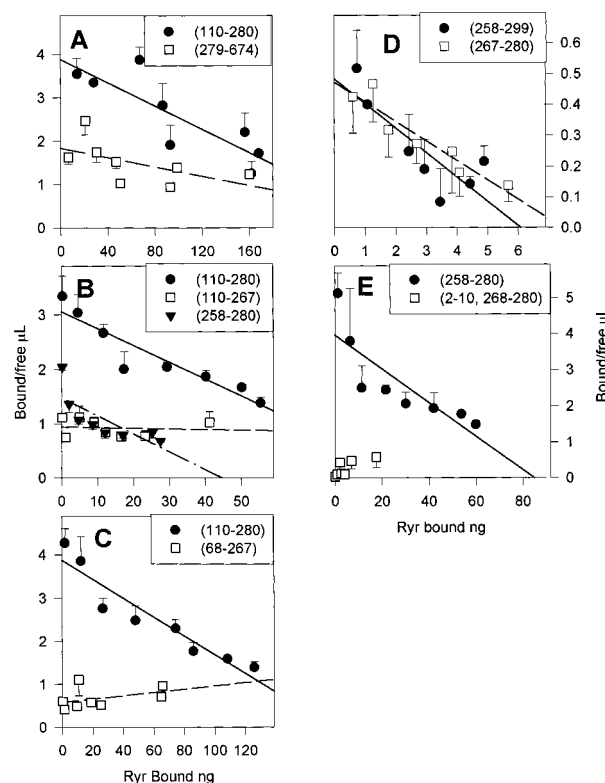


FIGURE 7: Scatchard plots of the binding of Ryr to various triadin constructs. The methods of binding are described under Methods. The binding media contained 210 mM NaCl. In each experiment, the amount of expressed protein for each assay point was in the range of 500 ng. The plots and regression lines were obtained using Sigmaplot. The error bars are the standard errors of the means of triplicate assays in a single experiment.

affinity site is present which is diminished by the elevation of ionic strength. In contrast, the binding of Ryr to triadin(279–674) is lower in both media, is unaffected by the presence of cold Ryr, and is more strongly inhibited by elevated ionic strength. This pattern indicates that triadin(279–674) binds to Ryr through a low-affinity ionic interaction.

Figure 7 shows Scatchard plots of binding of Ryr to variants of the 110–280 and 279–674 fusion peptide constructs using the glutathione columns in the presence of 210 mM NaCl. This relatively high ionic strength medium was chosen to unmask the high-affinity binding shown in Figure 6. Figure 7A shows a binding experiment comparing the two parent constructs. In this experiment, the 110–280 construct binds with considerably higher affinity (K_D 63 $\mu\text{g}/\text{mL}$) than the 279–674 fusion peptide (K_D 214 $\mu\text{g}/\text{mL}$). These values correspond to molar K_D s of 30 and 100 nM, respectively, assuming binding of one Ryr tetramer to the triadin peptide, confirming the observations of Figure 6.

Since the Western blot overlays had indicated a stronger binding of Ryr to triadin(279–674) than triadin(110–280) and triadin(110–267), we tested the latter construct further by comparing triadin(110–280) with triadin(110–267) which did not contain the hydrophobic region surrounding cysteine 270 (Figure 1). In this experiment, Ryr binds to triadin(110–280) with a K_D of 27 $\mu\text{g}/\text{mL}$ which is in the same range as that described in Figure 7A. The omission of residues 267–280 (open squares) caused the loss of the high-affinity Ryr binding site. Triadin(110–267) resembles triadin(279–674)

in binding to the Ryr with a weak interaction at a relatively high number of sites. In contrast, the short peptide, triadin(258–280), binds Ryr with high affinity but a relatively low number of binding sites (K_D 25 $\mu\text{g/mL}$). The binding properties of triadin(110–280) thus appear to be composed of two components: a low-affinity component of the bulk hydrophilic portion and a high-affinity component of the short peptide region from 267 to 280. One would expect that triadin(110–280) would contain both high- and low-affinity binding sites indicated by a flattening of the curve at high Ryr concentrations. Experimental limitations on the yield of Ryr from the muscle do not permit us to test this assumption.

The high-affinity binding of triadin(258–280) raises the question as to whether other short hydrophobic segments of triadin bind similarly to the Ryr. The hydrophobic residues 666–674 are contained in triadin(279–674) which does not bind with high affinity. The peptide triadin(68–267) contains the hydrophobic residues 102–111, but no other hydrophobic segment. Figure 7C compares this construct with triadin(110–280). Triadin(68–267) shows detectable, but only low-affinity, binding. The slope of this line is flat, indicating an indeterminate, but very high, K_D . On the other hand, the negative slope of the line of triadin(110–280) again indicates high-affinity binding.

Figure 7D,E characterizes further the hydrophobic segment 267–280. Triadin(267–280) (Figure 7D) contains only the amino acids in the hydrophobic region immediately adjacent to the cysteine, while triadin(258–299) contains some C-terminal amino acids adjacent to the hydrophobic region. The constructs give a binding K_D of 15 and 29 $\mu\text{g/mL}$, respectively. The binding of triadin(267–280) demonstrates that this minimal construct contains the necessary components of high-affinity binding and that the amino acids immediately surrounding 267–280 exert little influence on the strength of binding.

A third short construct that contains the putative binding region was prepared from triadin(2–280) by excision of amino acids 11–267 using two in-frame *NsiI* restriction sites in the cDNA. This fusion peptide, therefore, contains the N-terminal nine amino acids of triadin in addition to the hydrophobic Ryr binding segment. Figure 7E shows binding of this construct in comparison to triadin(258–280). The introduction of heterologous amino acids N-terminal to the binding region completely destroys binding to the Ryr (open squares). This observation indicates that the binding site on the Ryr can be impeded by a short length of inappropriate amino acids, suggesting that binding requires an exact fit between the sites on the two proteins.

The low number of high-affinity binding sites of some of the triadin constructs together with technical difficulties in assaying very small quantities of resin reproducibly has caused some scatter in the Scatchard plots. We have, therefore, averaged the K_D from separate experiments of all similar constructs in order to obtain a better estimate of the true binding constants. The K_D for those constructs designated by the open line in Figure 1 was $271 \pm 158 \mu\text{g/mL}$ ($n = 8$) while the K_D for long triadin constructs that contain residues 267–280 was $42 \pm 9 \mu\text{g/mL}$ ($n = 8$). The average K_D for all constructs shorter than 42 triadin amino acids that contain residues 267–280 was $20 \pm 4 \mu\text{g/mL}$ ($n = 4$). Student's *t* test indicates no significant difference between the affinities of the short and long constructs that contain residues 267–

280 ($P = 0.26$), while long constructs which do not contain these residues have significantly different affinities from those that do ($P = 0.045$) and from the short constructs that do ($P = 0.0023$).

DISCUSSION

In these experiments, we have employed two basic methods to detect and evaluate binding between triadin peptides and Ryr. Both Western blot overlay and affinity binding of Ryr to fusion peptides attached to a glutathione column give essentially similar evidence of a relatively low-affinity binding between the Ryr and extensive portions of triadin, which is eliminated at high ionic strength. On the other hand, only the affinity support binding demonstrates the presence of a high-affinity binding reaction between the Ryr and a short peptide from triadin. The reasons for the different specificities of the two methods are not clear, but each has some limitations. The Western blot overlay contains a step of denaturation of the triadin peptide in SDS, followed by removal of the detergent during transfer to the membrane. The binding to the Immobilon membrane depends on nonspecific interactions between the fluorocarbon membrane and the protein. It is possible that the relatively hydrophobic high-affinity binding region of triadin interacts directly with the membrane and thereby occludes it from the Ryr. In the affinity assay, the construct is attached to the support through the strong binding of the glutathione transferase to glutathione on the column. The inserted triadin sequence is separated from the GST by a 27 amino acid sequence culminating in 5 glycines. These offer the opportunity for the insert to segregate away from the support and to hinge around the oligoglycine residues. The Ryr is a bulky molecule that may not have the flexibility to expose a specific binding site in the constricted environment of the membrane filter while being accessible to a fusion peptide which can rotate away from its attachment point. These arguments indicate that the binding may be better observed when both proteins are in solution; however, we have found that many of the triadin peptides have limited solubility, except in media of high ionic strength.

The low-affinity sites have been observed using both experimental protocols. Binding has been observed not only for intact triadin but also for several expressed peptides. The binding of triadin(110–267) and triadin(279–674) to Ryr appears to be similar even though the peptides contain no overlapping sequence. This suggests either that both peptides have a common motif or that the properties required for binding are of a general character. Although both segments contain repetitions of the sequence KKEEK or minor variants, the most general point of similarity between them is their large charge content and extensive domain of net positive charge. The Ryr has a considerable excess of net negative charges so that the low-affinity interaction might arise from simple charge attraction. This is consistent with the strong influence of ionic strength on the binding.

The low-affinity triadin peptides appear to have a large maximum number of Ryr binding sites. This could arise if several molecules of Ryr bind to a single triadin molecule. The gels of the expressed peptides on the glutathione column each contain on average approximate 500 ng of protein. On a molar basis, the capacity of the triadin peptides for the

Ryr is considerably in excess of the amount of Ryr used in each assay. However, the number of sites on the column available for interaction with the Ryr is likely to be much lower, since the peptides can bind to sites within the matrix of the beads from which the bulky Ryr is excluded. The large size of the Ryr probably precludes large numbers from binding to each triadin peptide even if the binding is of a general ionic nature. The very low number of high-affinity binding sites of triadin(110–280) and triadin(267–280) may be caused by the more stringent requirement of accessibility when only a single region of the Ryr binds to a single region of the peptide.

Binding studies of triadin to the Ryr have all been performed using extracted proteins and do not demonstrate that these proteins are able to attach to each other in situ. Of particular concern with triadin and the Ryr is that both proteins are intrinsic membrane proteins in which a membrane barrier may limit the interaction of regions of one protein from regions of the other. The topology of neither Ryr nor triadin is known unequivocally. Nevertheless, hydropathy plots and a number of antibody epitope studies have indicated that the membrane-spanning regions of the Ryr are confined to the C-terminal extremity, while the N-terminal bulk of the protein is cytoplasmic. Current models of Ryr structure indicate that the short acidic regions, 4583–4644 and 4855–4921, are luminal (29, 30). The large cytoplasmic unit contains a large excess of negative charges. There is general agreement that triadin(279–674) is luminal, while the locus of triadin(110–267) differs with different models. It is, therefore, feasible that low-affinity binding sites between triadin and the Ryr may occur in situ, although experimental studies will be needed to confirm this.

Similar concerns may be expressed concerning the interaction of triadin(267–280) with the Ryr, but the high specificity, the absence of net charge, the stringent conditions for binding, and the high affinity make it much less likely that this interaction is an artifact of isolated proteins. This binding region is an interesting part of the triadin molecule, since it is a short relatively hydrophobic region that contains one of the two cysteines that form the disulfide-linked polymer. The role of triadin polymerization in its function is not clear, but Liu et al. (31) have presented evidence for a link between thiols on the Ryr and triadin. The binding between triadin(267–280) could serve as the point of connection which allows thiol-disulfide exchange between these two proteins.

REFERENCES

1. Rios, E., and Brum, G. (1987) *Nature* 325, 717–720.
2. Tanabe, T., Takeshima, H., Mikami, A., Flockerzi, V., Takahashi, H., Kangawa, K., Kojima, M., Matsuo, H., Hirose, T., and Numa, S. (1987) *Nature* 328, 313–318.
3. Tanabe, T., Beam, K. G., Adams, B. A., Niidome, T., and Numa, S. (1990) *Nature* 346, 567–569.
4. Campbell, K. P., Knudson, C. M., Imagawa, T., Leung, T. T., Sutko, J. L., Kahl, S. D., Raab, C. R., and Madson, L. (1987) *J. Biol. Chem.* 262, 6460–6463.
5. Inui, M., Saito, A., and Fleischer, S. (1987) *J. Biol. Chem.* 262, 1740–1747.
6. Lai, F. A., Erickson, H. P., Rousseau, E., Liu, Q. Y., and Meissner, G. (1988) *Nature* 331, 315–320.
7. Block, B. A., Imagawa, T., Campbell, K. P., and Franzini-Armstrong, H. (1988) *J. Cell Biol.* 107, 2587–2600.
8. Takekura, H., Takeshima, H., Nishimura, S., Takahashi, M., Tanabe, T., Flockerzi, V., Hofmann, F., and Franzini-Armstrong, C. (1995) *J. Muscle Res. Cell Motil.* 16, 465–480.
9. Protasi, F., Franzini-Armstrong, C., and Allen, P. D. (1998) *J. Cell Biol.* 140, 831–842.
10. Powell, J. A., Petheridge, L., and Flucher, B. E. (1996) *J. Cell Biol.* 134, 375–387.
11. Lu, X., Xu, L., and Meissner, G. (1994) *J. Biol. Chem.* 269, 6511–6516.
12. Lu, X., Xu, L., and Meissner, G. (1995) *J. Biol. Chem.* 270, 18459–18464.
13. El-Hayek, R., and Ikemoto, N. (1998) *Biochemistry* 37, 7015–7020.
14. Leong, P., and MacLennan, D. H. (1998) *J. Biol. Chem.* 273, 7791–7794.
15. Brandt, N. R., Caswell, A. H., Wen, S.-R., and Talvenheimo, J. A. (1990) *J. Membr. Biol.* 113, 237–251.
16. Kim, K. C., Caswell, A. H., Talvenheimo, J. A., and Brandt, N. R. (1990) *Biochemistry* 29, 9281–9289.
17. Motoike, H. K., Caswell, A. H., Brandt, N. R., Brunschwig, J.-P., and Smilovitz, H. (1994) *J. Muscle Res. Cell Motil.* 15, 493–504.
18. Caswell, A. H., Brandt, N. R., Brunschwig, J.-P., and Purkerson, S. (1991) *Biochemistry* 30, 7507–7513.
19. Knudson, C. M., Stang, K. K., Moomaw, C. R., Slaughter, C. A., and Campbell, K. P. (1993) *J. Biol. Chem.* 268, 12646–12654.
20. Peng, M., Fan, H., Kirley, T., Caswell, A. H., and Schwartz, A. (1994) *FEBS Lett.* 348, 17–20.
21. Fan, H., Brandt, N. R., Peng, M., Schwartz, A., and Caswell, A. H. (1995) *Biochemistry* 34, 14893–14901.
22. Knudson, C. M., Stang, Jorgensen, A. O., and Campbell, K. P. (1993) *J. Biol. Chem.* 268, 12637–12645.
23. Marty, I., Robert, M., Ronjat, M., Bally, I., Arlaud, G., and Villaz, M. (1995) *Biochem. J.* 307, 769–774.
24. Fan, H., Brandt, N. R., and Caswell, A. H. (1995) *Biochemistry* 34, 14902–14908.
25. Guo, W., and Campbell, K. P. (1995) *J. Biol. Chem.* 270, 9027–9030.
26. Carl, S. L., Felix, K., Caswell, A. H., Brandt, N. R., Brunschwig, J.-P., Meissner, G., and Ferguson, D. G. (1995) *Muscle Nerve* 18, 1232–1243.
27. Caswell, A. H., Lau, Y. H., and Brunschwig, J.-P. (1976) *Arch. Biochem. Biophys.* 176, 417–430.
28. Ron, D., and Dressler, H. (1992) *BioTechniques* 13, 866–869.
29. Takeshima, H., Nishimura, S., Matsumoto, T., Ishida, H., Kangawa, K., Minamino, Matsuo, H., Ueda, M., Hanaoka, M., Hirose, T., and Numa, S. (1989) *Nature* 339, 439–445.
30. Zorzato, F., Fujii, J., Otsu, K., Phillips, M., Green, N. M., Lai, F. A., Meissner, G., and MacLennan, D. H. (1990) *J. Biol. Chem.* 265, 2244–2256.
31. Liu, G., and Pessah, I. N. (1994) *J. Biol. Chem.* 269, 33028–33034.

BI981306+